JOURNAL OF COLLOID AND INTERFACE SCIENCE **180,** 590–597 (1996)
ARTICLE NO. 0340

Extended Characterization of Combustion-Generated Aggregates: Self-Affinity and Lacunarities

ALEXANDER V. NEIMARK,[1] ÜMIT Ö. KÖYLÜ, AND DANIEL E. ROSNER

Department of Chemical Engineering, Yale University, New Haven, Connecticut 06520-8286

Received August 25, 1995; accepted December 27, 1995

A large population of combustion-generated soot aggregates (more than 3000 samples) was thermophoretically extracted from a variety of laminar and turbulent flames and analyzed by using transmission electron microscopy (TEM). It was shown that the scaling structural properties of these fractal aggregates *cannot* be exclusively characterized by a single mass fractal dimension. Asymmetric properties of the aggregates were considered here by first assuming and then demonstrating their *self-affinity* via affinity exponents reflecting different scaling with respect to the length and width of the aggregate projections. In addition to the conventional fractal dimension, D_f, determined by using the geometrical mean of the longitudinal and transverse sizes as the characteristic length, the affinity exponent, H, and two complementary fractal dimensions, one longitudinal, $D_L = [(1 + H)/2]D_f$, and one transverse, $D_W = [(1 + H)/2H]D_f$, were introduced. By fitting the TEM data for the entire population of aggregates, the values of $D_f = 1.75$ and $H = 0.91$ were obtained. To classify the density and crossover scales of aggregates having the same fractal dimensions, lacunarities of the first and second order were also defined as prefactors in the scaling relationships among aggregate mean mass, rms mass and linear sizes. Analysis of the second moment of the mass-size distribution confirmed that the scaling properties of flame-generated aggregates cannot be consummately characterized by a single fractal dimension; it is necessary to introduce a set of scaling exponents. This more precise description of aggregate morphologies in terms of self-affine scaling and lacunarities is not captured by previous idealized cluster–cluster aggregation models. Current investigations of the reasons for this are expected to lead to a deeper understanding of the coagulation dynamics, transport properties, and restructuring kinetics of flame-generated aggregates.

Key Words: **aggregates; combustion; fractals; aggregation; morphology.**

INTRODUCTION

Fractal aggregates and patterns are produced in many engineering and natural environments. Although their morphology may look very complex, they are usually well-characterized by a single structural parameter, namely, the mass fractal dimension, D_f (1–3). Moreover, the products of aggregation and pattern formation are divided into a few ''universality'' classes, each characterized by a certain value of D_f. The most practically important universality classes are diffusion-limited aggregation (DLA), diffusion-limited cluster–cluster aggregation (DLCCA), ballistic cluster–cluster aggregation (BCCA), reaction-limited cluster–cluster aggregation (RLCCA), and percolation clusters (PC). It has been supposed that the fractal dimension, D_f, reflects the main features of the pattern formation procedure. For example, products of DLA are characterized by fractal dimensions ca. 1.7 in two-dimensions (2D) and ca. 2.5 in 3D, despite the variety of different physical phenomena and experimental conditions which formally fit the classical Witten–Sander model (4) (electrodeposition (5), viscous fingering in porous media (6), dendritic growth (7), deposition on surfaces (8), diffusion-limited polymerization (9), dielectric breakdown (10), dissolution of porous media (11), etc.). It is worth noticing that the fractal dimension of 3D PC coincides very closely with that of 3D DLA patterns. The products of DLCCA constitute another universality class, characterized by fractal dimensions ca. 1.43 in 2D and ca. 1.78 in 3D. Typical examples of DLCC aggregates are liquid-phase products such as colloidal gold (12) and gas-phase products such as aggregates of metal particles in a dense vapor (13), or flame-generated aggregates (carbonaceous soot (14), alumina aggregates (15)). The latter are the main focus of experimental part of this paper, where it will be shown that real combustion aggregates exhibit systematic morphological differences from those predicted by idealized DLCCA simulation models. The fractal dimension of computer-generated BCC aggregates, as expected in a low-density gas, is slightly higher—ca. 1.9 for 3D aggregates. Conditions leading to BCCA are realized in some combustion processes (16). Even more dense structures are characteristic for RLCCA, with fractal dimensions greater than 2 in 3D. The universal fractal dimension of 2.1 has been found for three completely different colloids: gold, silica, and polystyrene (17). This means that the 2D projections of RLCC aggregates are not fractals and form 2D compact patterns.

[1] To whom correspondence should be addressed.

0021-9797/96 $18.00

Products of cluster–cluster aggregation can be obtained in gas and liquid phases in different engineering environments and sometimes under transition conditions among DLCCA, BCCA, and RLCCA. Therefore, with a few exceptions, the experimental values of fractal dimensions vary mostly between 1.6 and 2.2. Other typical examples of fractal aggregates are aerogels (18), titanium oxide (19), carbon black (20), silica (21), etc.

Mass fractal dimension D_f is defined as the dimensionless exponent in a scaling relationship between the total number (or mass) of primary particles, N, and linear size of aggregates, R, ''reduced'' by the primary particle radius, a_p:

$$N = \alpha_R (R/a_p)^{D_f}. \quad [1]$$

The coefficient α_R, denoted by Mandelbrot (1) as a first-order *lacunarity*, is a complementary structural parameter characterizing the aggregate density and cutoff of fractality. In practical fractal analysis, lacunarities have been seldomly used, with most attention being traditionally paid to fractal dimensions. Nevertheless, a range of so-called fractal prefactors (read lacunarities) were reported for the characterization of thermophoretically sampled carbonaceous soot aggregates by Sorensen *et al.* (22), Puri *et al.* (23), Cai *et al.* (24), and Köylü *et al.* (25). Recently, Köylü *et al.* (26) found that both values of fractal dimension and fractal prefactor were ''universal'' for different carbonaceous soot and alumina aggregates using angular light scattering as well as analysis of transmission electron microscope (TEM) images. Moreover, as emphasized by Sorensen *et al.* (22) and Köylü *et al.* (26), the fractal prefactor is essential to properly interpret *in situ* light-scattering measurements in particle-laden reacting systems. Significant for the present paper, Köylü *et al.* (26) pointed out that the observed first-order lacunarity for flame-generated aggregates is systematically higher (by ca. factor of 2) than that ''anticipated'' based on the above-mentioned cluster–cluster aggregation simulation models.

It is usually assumed that Eq. [1] is valid for any characteristic linear size of the aggregate, and in contrast to the prefactor/lacunarity the choice of this size does not affect the inferred fractal dimension. This is one consequence of a proposed *self-similarity* of aggregates. Theoretically, the most straightforward choice is to use the radii of gyration of aggregates. However, for 3D aggregates with $D_f < 2$, comprised of small spherical particles, while projected lengths and primary particle radii are easily obtained from TEM data by analyzing 2D projections of the aggregates, the radius of gyration can not be measured directly. Instead, following the pioneering work of Weitz and Huang (12), the geometric mean $(LW)^{1/2}$ of the length of the longest axis, L, and the width, W, of the aggregate projection measured perpendicular to this axis is commonly employed as the characteristic linear size to be used in the scaling relationship of Eq. [1] for defining fractal dimensions, i.e.,

$$\langle N \rangle = \alpha((LW)^{1/2})^{D_f}. \quad [2]$$

Here $\langle \cdots \rangle$ denotes averaging over aggregates with given length L and width W of the plane projection. Note here that the length L and width W are dimensionless; i.e., they are measured in multiples of the mean primary particle diameter. The structural parameters, lacunarity α and ''geometric mean'' fractal dimension, D_f, are then obtained by using least-squares fitting for a given population of fractal aggregates, or, more precisely, for a given set of TEM images.

In previous papers of Botet and Jullien (27), and Lindsay *et al.* (28), the anisotropic properties of cluster–cluster aggregates were discussed based on the results of numerical simulations. The simulated aggregates were essentially found to be anisotropic, however the anisotropic structural parameters were scale-invariant and could be expressed in terms of self-similarity. The main goal of this paper is to consider in greater detail the morphological regularities of aggregates found in flames. Based on a statistical analysis of a large population of combustion-generated carbonaceous soot aggregates (more than 3000 samples), we have critically examined the hypothesis of self-similarity using samples thermophoretically extracted from a wide variety of laboratory flames. We show here that flame-generated aggregates must be considered as *self-affine* (rather than self-similar) objects. Moreover, analysis of the second moment of the aggregate mass-size distribution reveals that it is necessary to introduce a set of exponents to characterize scaling properties of such aggregates (3). Different exponents, and first- and second-order lacunarities, are introduced for the more detailed characterization of such fractal aggregates. We raise the fundamental question: What feature(s) of the flame environment are responsible for these systematic departures between real aggregates and those anticipated from idealized cluster–cluster aggregation (CCA) models?

EXPERIMENTAL METHODS

Since the present study deals mainly with the detail characterization of combustion-generated aggregates, the following description of the experimental procedures is brief, and additional details can be found in Köylü and Faeth (29, 30), and Sunderland *et al.* (31).

Thermophoretic sampling procedures to extract representative aggregates from flame environments were based on the experimental and theoretical methods established by Dobbins and Megaridis (32) and Rosner *et al.* (33), respectively, and extensively used by Köylü and Faeth (29). The sampling surfaces were carbon-supported copper grids used to hold TEM specimens (3 mm diameter 200 mesh copper grids), aligned parallel to the mean flow direction. The probes were stored outside the flames and inserted briefly into the flame environment using a double-acting pneumatic cylinder. Sampling times were 30–100 ms in order that the

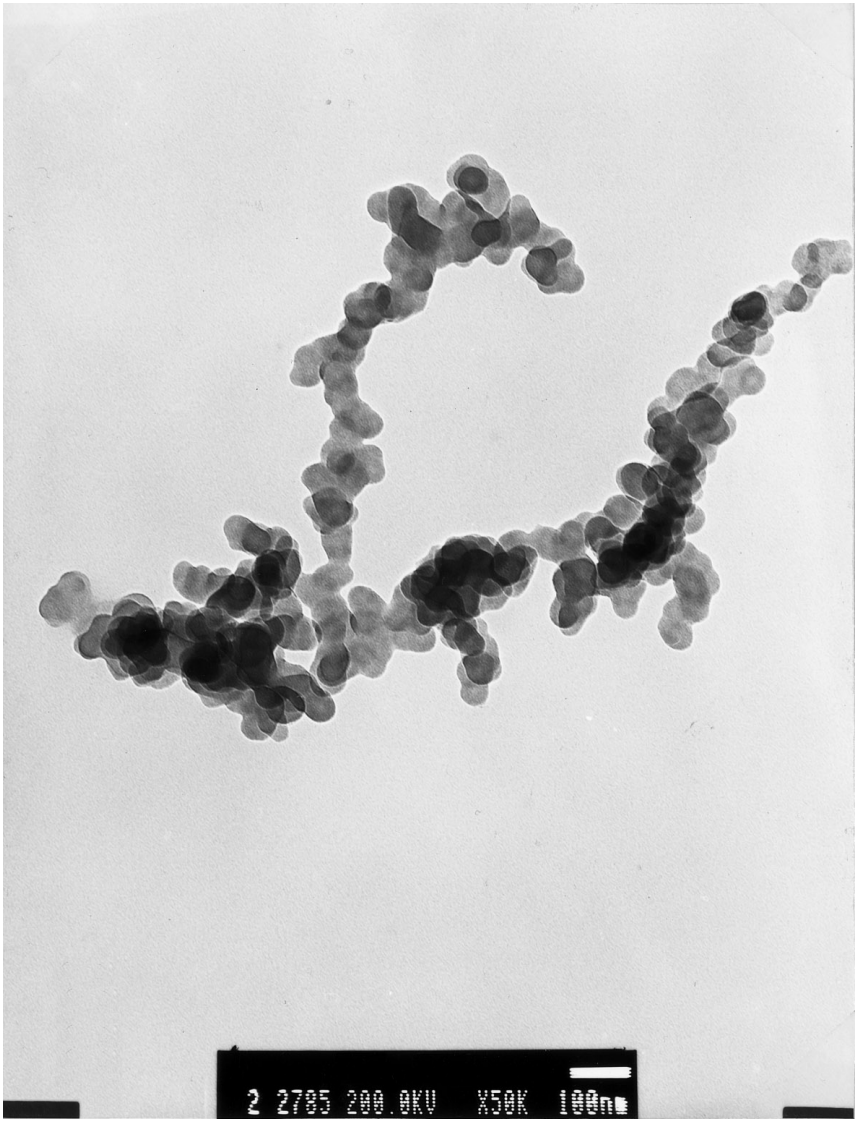

FIG. 1. TEM photograph of a typical combustion-generated carbonaceous soot aggregate thermophoretically sampled from a turbulent acetylene/air diffusion flame.

collected soot aggregates cover no more than 10% of the TEM grid. This avoided overlapping of aggregates on the grid.

The samples were observed using a JEOL 2000FX analytical electron microscope system with a 1-nm edge-to-edge resolution. Magnifications used for the present measurements were in the range $0.6-30 \times 10^4$. The procedure involved selecting aggregates randomly at low magnification, and then increasing the magnification in order to analyze them. The images were processed on a computer to find aggregate areas and geometric dimensions, as well as the sizes of primary particles. A typical carbonaceous soot aggregate sampled from a turbulent acetylene flame is shown in Fig. 1. Primary particle sizes in a set of aggregates sampled from a particular flame condition can usually be represented by a single mean radius, a_p, due to narrow size distributions with standard deviations generally less than 20% of the mean values. Since $D_f < 2$, the number of primary particles, N, in an aggregate was estimated from an empirical correlation between aggregate and particle projected areas by means of a procedure described elsewhere (25, 26).

The TEM measurements involved thermophoretic sampling of carbonaceous soot aggregates from a variety positions in different diffusion flame environments, including the nonluminous (overfire) region of buoyant turbulent flames fueled with gases (acetylene, propylene, ethylene, propane) or liquids (toluene, benzene, n-heptane, isopropanol) (29), luminous (fuel-rich) region of buoyant laminar flames fueled with acetylene or ethylene (30), and of a weakly buoyant acetylene flame operating at $\frac{1}{4}$ atm (31). These various exper-

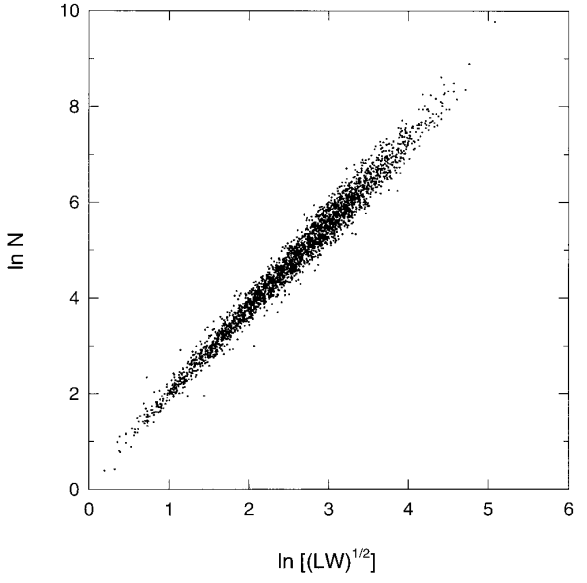

FIG. 2. Number of primary particles, N, in aggregates as a function of the characteristic length, $(LW)^{1/2}$ for a population of 3080 carbonaceous soot aggregates thermophoretically sampled from various diffusion flame environments, yielding the fractal dimension, D_f.

imental conditions resulted in an aggregate population of 3080 images, which were analyzed following the specific methods of Köylü *et al.* (25, 26). Experimental uncertainties (95% confidence interval) of aggregate morphological parameters obtained from TEM images were estimated to be generally less than 1–2% due to our large population of 3080 aggregates.

RESULTS AND DISCUSSION

Self-Affinity of Fractal Aggregates

The scaling relationship [2] is valid for the combustion-generated aggregates under consideration. Figure 2 illustrates number of primary particles in aggregates, N, as a function of characteristic linear size, $(LW)^{1/2}$, with the least-squares fit to data yielding[2] the fractal dimension $D_f = 1.75 \pm 0.01$ that is typical for DLCCA. TEM images (see Fig. 1) show that the aggregate shapes are mostly asymmetric, and the aggregate projections are almost always elongated, with the length and width being considerably different. The aspect ratio L/W is found to vary in random fashion between 1 and 4, tending to increase with increased aggregate size. This observation suggests that the aggregates may be *self-affine* rather that self-similar. Supposition of statistical self-affinity implies that the aggregate shape is invariant (in a statistical sense) with respect to anisotropic scaling transformations (see, for example, (34–36), i.e., with respect to shrinking or stretching with different scaling factors, n_L and n_W, in the longitudinal and transverse directions:

$$L \to n_L L; \quad W \to n_W W. \qquad [3]$$

Thus, the length L and width W of self-affine aggregates are related through the so-called affinity exponent, H, defined as a ratio of the logarithms of longitudinal and transverse scaling factors (35):

$$H \equiv \ln(n_W)/\ln(n_L). \qquad [4]$$

Accordingly, an increase in length by the factor n is associated with an increase in width by the factor n^H, so that, on the average,

$$W = W_0(L/L_0)^H. \qquad [5]$$

Here L_0 and W_0 are the longitudinal and transverse dimensions of some reference aggregate.

For self-affine systems the affinity exponent is less than unity, $H < 1$, and it follows from Eq. [5] that with an increase in size the aggregates tend to become more and more elongated. For self-similar systems, $H = 1$ and the aggregate *shape* is invariant with respect to isotropic scaling transformations. In other words, length and width are directly proportional only for self-similar aggregates.

Self-affinity of the aggregates under consideration is our conjecture, and is demonstrated below. It is worth noticing that invariance with respect to anisotropic scaling transformations does not always ultimately imply self-affinity. In botany and biology, anisotropic scaling invariance [3] is known as one kind of allometry (see, e.g., Stahl (37); Mandelbrot (1, p. 350)) and dates back to Galileo (38). The most prominent example of allometry is an observation that the ratio of botanical tree height cubed over its trunk diameter squared is constant. This suggests allometric similitude of trees: if tree heights differ by factor n then their trunk diameters differ by $n^{3/2}$.

Self-affinity implies more than geometric allometry. It implies hierarchical structure of given objects. Self-affine objects can be decomposed into non-overlapping parts, each of which is similar to the whole with respect to the anisotropic scaling transformation (3). Thus, to check self-affinity of the aggregates, one must prove anisotropic invariance for the constituent parts of the aggregates. Because experimentally this is hardly feasible, the only practical approach is to test the scaling properties of the entire aggregates themselves rather than their parts. When we use the term ''self-affinity'' for combustion-generated aggregates, our conjecture is that, because they are the products of cluster-cluster aggregation, each of them is comprised of smaller aggregates/clusters

[2] Here and below, the margin of error is calculated using the standard method of random uncertainty with a confidence level of 95%.

which are statistically similar to some aggregates represented in our population. In other words, any aggregate in the population can be considered as a potential constituent part of a larger aggregate. This means that, instead of studies of scaling properties of the constituent parts of the aggregates, the sought results can be obtained by considering scaling properties of the aggregates themselves.

It is well known (35) that, contrary to a self-similar system (whose scaling properties are characterized by a single parameter called fractal dimension), for a self-affine system a multitude of different fractal dimensions can be introduced depending on the definition of the aggregate characteristic size. In particular, the conventional ''geometric mean'' fractal dimension D_f defined in Eq. [2] was introduced by Mandelbrot (35) as ''gap'' dimension. Considering scaling relationships with respect to aggregate length and width taken separately, one is led to the following definitions, which represent the lengthwise and widthwise scaling:

$$\langle N\rangle = \alpha_L L^{D_L}. \quad [6]$$

Here the ''longitudinal'' fractal dimension D_L is introduced together with its associated ''longitudinal'' lacunarity α_L, and

$$\langle N\rangle = \alpha_W W^{D_W}, \quad [7]$$

where the ''transverse'' fractal dimension D_W is introduced together with its associated ''transverse'' lacunarity α_W.

In general, any combination of length and width, $L^\gamma W^{1-\gamma}$, can be employed as characteristic aggregate size, and the corresponding fractal dimension, D_γ, with its associated lacunarity, α_γ, can be defined by

$$\langle N\rangle = \alpha_\gamma (L^\gamma W^{1-\gamma})^{D_\gamma}. \quad [8]$$

The fractal dimensions, D_f, D_L, and D_W, defined above are particular cases of D_γ at $\gamma = \frac{1}{2}$, 1, and 0, respectively. By combining Eqs. [5] and [8], the following relationship is obtained:

$$\langle N\rangle = \alpha_\gamma (L^\gamma W^{1-\gamma})^{D_\gamma} = \alpha((LW)^{1/2})^{[(\gamma+H(1-\gamma))/((1+H)/2)]D_\gamma}. \quad [9]$$

Thus, the conventional ''geometric mean'' or ''gap'' fractal dimension D_f defined in Eq. [2] is related to the fractal dimension D_γ defined in Eq. [6]:

$$D_f = [(\gamma + H(1-\gamma))/((1+H)/2)]D_\gamma. \quad [10]$$

By taking D_f as a reference, the longitudinal D_L and D_W transverse fractal dimensions can be expressed as follows:

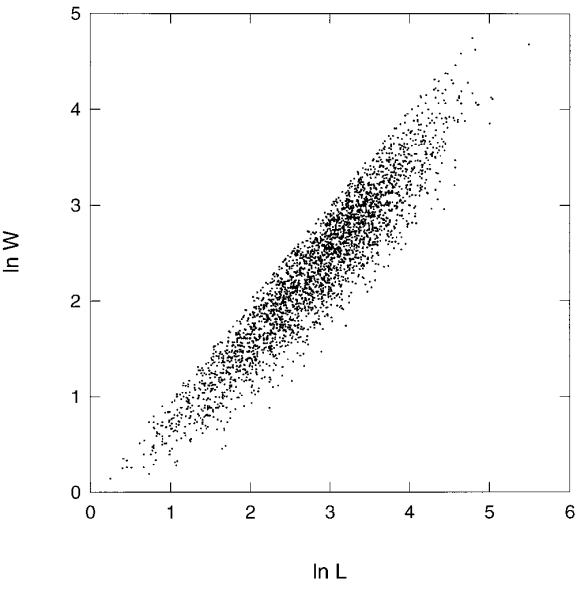

FIG. 3. Width, W, perpendicular to the maximum projected length as a function of this longest axis, L, of aggregates for carbonaceous soot aggregates from various diffusion flame environments, yielding the affinity exponent, H (Eq. [4]).

$$D_L = [(1+H)/2]D_f; \quad D_W = [(1+H)/2H]D_f. \quad [11]$$

These general scaling relationships for self-affine systems described above were verified for our population of combustion-generated thermophoretically sampled aggregates. The least-squares fitting of Eq. [5] with regard to the whole population of 3080 soot aggregates yielded the affinity exponent $H = 0.91 \pm 0.01$ (see Fig. 3). The data presented in Fig. 3 show that there is a relatively wide distribution of aggregate widths at a particular aggregate length. Therefore, a correlation between the averaged width, $\langle W(L)\rangle$, and the length, L, is presented in Fig. 4. This plot was constructed by dividing the length scale into equal intervals and averaging the widths within each length interval. Although this procedure is somewhat arbitrary, the resulting plot is more instructive than Fig. 3 since the data scatter is reduced. Consequently, the anisotropic scaling is clearly visible. The least-squares analysis of Fig. 4 yielded the self-affinity exponent $H = 0.89 \pm 0.02$, which is necessarily identical to the value obtained from the statistical analysis of the initial experimental data shown in Fig. 3. Thus, using this H value and $D_f = 1.75$, Eq. [11] predicts noticeably different values for the ''longitudinal'' and ''transverse'' fractal dimensions: $D_L = 1.67$, and $D_W = 1.83$. On the other hand, the corresponding experimental values, obtained formally by the least-squares fittings of Eqs. [6] and [7] with regard to the whole population of soot aggregates, are $D_L = 1.68 \pm 0.01$, and $D_W = 1.72 \pm 0.01$. The experimental value of D_L is in perfect agreement with the predicted one, whereas the experimental value of D_W is about 7% smaller than the theoretical predic-

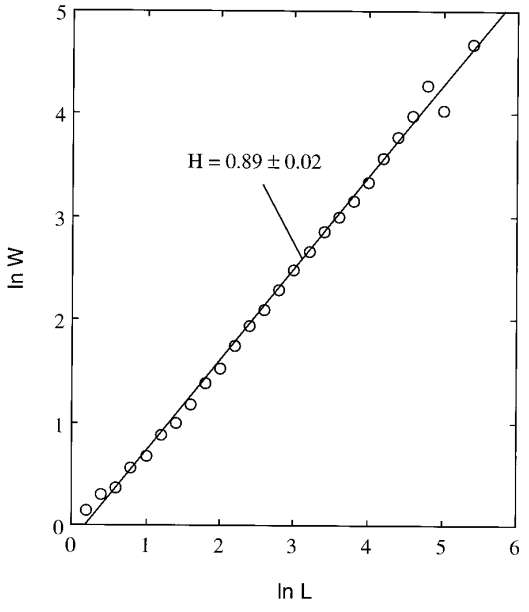

FIG. 4. Average width, $\langle W \rangle$, as a function of length, L, for the original ''raw'' data shown in Fig. 3. The plot was constructed by dividing the length scale into equal intervals and averaging the widths within each length interval.

tion. This latter deviation may be attributable partially to the experimental definition of the width, W, of aggregate projections which leads to substantially larger uncertainty in W than in L (e.g., $D_W = 1.8$ gave the mean square deviation only ca. 4% larger than the least square deviation obtained at $D_W = 1.72$). Thus, we conclude that *combustion-generated soot aggregates should be regarded as self-affine rather than self-similar*. Possible implications of this intrinsic ''asymmetry,'' not captured in previously used cluster–cluster aggregation models, will be considered briefly below.

Lacunarities

Lacunarities, introduced as prefactors in the mass-size scaling relationships, are valuable structural parameters complementary to fractal dimensions and scaling exponents. The lacunarity characterizes density and cutoff scales of fractals (1). For aggregates to be self-similar above a lower cutoff scale, a_b, their morphology can be regarded as being comprised of renormalized units, or ''blobs,'' of size a_b, which are formed from primary particles. The volume density of blobs, ρ_b is finite, and the number of primary particles in the blob $N_b = \rho_b(a_b/a_p)^D$, where a_p is the size of primary particles and D is the spatial dimension ($D = 2$ in 2D, and $D = 3$ in 3D). The number of blobs in an aggregate of size R scales as $(R/a_b)^{D_f}$. Thus, Eq. [1] can be expressed as follows:

$$N = \alpha(R/a_p)^{D_f} = \rho_b(a_b/a_p)^D(R/a_b)^{D_f}.$$

Here the lacunarity is

$$\alpha = \rho_b(a_b/a_p)^{D-D_f}. \quad [12]$$

One would expect that within one universality class, aggregates produced in different environments and having the same fractal dimension may have different lacunarities. The lacunarity represents the local structure of aggregates at scales comparable with the size of primary particles. Local structural properties, i.e., local density and blob size, may depend on synthesis conditions, e.g., interparticle sintering, contact deformations, etc. In general, larger lacunarities correspond to higher density aggregates.

Lacunarities can be defined based on any mass-size scaling relationship, including the self-affine one [8]. The lacunarities defined using different linear sizes are, of course, interrelated. Note that for stochastic populations of aggregates, these scaling relationships contain the average mass $\langle N \rangle$, or the first moment of mass-size distribution. For this reason, the corresponding lacunarities are referred to as the first-order lacunarities.

The second-order lacunarity was defined by Mandelbrot (1) from scaling of the second moment of the aggregate mass-size distribution. In a similar way, it is possible to introduce second-order geometric mean lacunarities from the following scaling relationship:

$$\langle \{ [N(L, W) - \langle N(L, W) \rangle]^2 \} \rangle^{1/2} = \alpha_2 [(LW)^{1/2}]^{D_{2,f}}. \quad [13]$$

The exponent in Eq. [13] may differ from the corresponding exponent obtained from the first moment relationship, Eq. [2]. Only in the special case of a self-similar system are they identical. In general, a deviation between D_f and $D_{2,f}$ points to what is called *multifractality* (1, 3). Sometimes, the term *generalized dimensions* is used for exponents obtained from higher moment correlations (3). We do not use this term for $D_{2,f}$ since it might be somewhat misleading because the above definition [13] differs from the conventional definition of generalized dimensions for multifractal measures on a fractal set (3). A multifractal formalism for the description of aggregate populations is still in progress.

First and second order lacunarities and fractal dimensions, determined from our population of carbonaceous soot aggregates, are summarized in Table 1. The second-order exponent $D_{2,f}$ differs somewhat from the first-order one, and, therefore, we conclude that the scaling properties of combustion-generated aggregates cannot be completely described either by one fractal dimension D_f (as would be the case for ideal self-similar fractals) or even by two scaling exponents D_f and H (as would be the case for ideal self-affine fractals), but rather by a set of exponents, characteristic of self-affine multifractal systems (3). Nevertheless, because the deviations of these aggregates from ideal self-similar fractals are generally less than 10%, and relatively high ex-

TABLE 1
Structural Parameters of Combustion-Generated Carbonaceous Soot Aggregates

Fractal property	Experimental value (least-squares fit)	Uncertainty interval (95% confidence)
α	1.33	0.02
D_f	1.75	0.01
H	0.91	0.01
α_2	0.06	0.01
$D_{2,f}$	2.00	0.05

perimental uncertainties associated with determining the second-order lacunarity, a single mass fractal dimension together with the first-order lacunarity may still be practically useful for characterizing the orientation-averaged transport properties of combustion-generated aggregates.

Practical Implications

The anisotropic scaling properties observed in our work, as well as the underprediction of first-order lacunarity recently reported by Refs. (25) and (26), suggest that the ideal model of DLCCA does not adequately describe the mechanism of particle aggregation in flames. This immediately raises the important question: what physical phenomena currently absent in these idealized computer simulations must now be taken into account? Most likely, the intrinsic anisotropy of the local environment in particle-producing flames affects aggregate morphology. Additional causes of aggregate anisotropy, currently under investigation, may be the electrostatic repulsion of the aggregates undergoing collisions. Electrostatic repulsion should be smaller for aggregate collisions with smaller interaction areas, i.e., repulsion is smaller when the distance between the centers of gyration of the colliding particles is maximized. This would lead to the relative elongation of aggregates after coagulation. The anisotropic structural properties of combustion-generated aggregates should also be reflected in some of their transport properties, especially prior to orientation-averaging. To date, several important transport properties of large fractal aggregates have been estimated via quasi-continuum methods exploiting the assumption of a quasi-spherical shape (39, 40), in part based on the notion that this might be an adequate approximation for *orientation-averaged* properties. However, it is well known from both experimental and theoretical studies that the effect of nonsphericity should be taken into account in predicting viscous drag, dynamic mobility, and sedimentation, especially for applications in which all orientations are *not* equally probable (see, for example, (41–45) and references cited therein). The self-affinity established in this study can be used to modify some of these relationships, derived previously for symmetric particles, to apply more accurately to large ''asymmetric'' fractal aggregates.

The associated lacunarities (prefactors) can be helpful in modeling aggregate *restructuring* due to, for example, sintering. Such processes lead to the ''collapse'' of aggregates and, in particular, to an increase in local density and associated lacunarity. Although the theoretical models that have recently been applied to quasi-spherical particles (46) could be used for studies of restructuring on the level of blobs, a scaling approach as suggested by this study should be developed for considerations on the level of aggregates.

SUMMARY AND CONCLUSIONS

Using the prominent example of thermophoretically sampled combustion-generated aggregates, it was shown that the scaling structural properties of DLCCA products cannot be characterized solely by using the now-familiar mass fractal dimension, D_f. The asymmetric properties of flame-generated aggregates were characterized here by first assuming and then verifying their *self-affinity*, introducing different exponents reflecting a scaling invariance with respect to the length and width of the aggregate projections. The affinity exponent, H, and two complementary fractal dimensions, one longitudinal, $D_L = [(1 + H)/2]D_f$, and one transverse, $D_W = [(1 + H)/2H]D_f$, were introduced. By fitting our TEM experimental data for the entire population of 3080 carbonaceous soot aggregates, the values $D_f = 1.75$ and $H = 0.91$ were obtained, and it has been demonstrated that this departure of H from unity is statistically significant. We note that widely employed diffusion-limited cluster–cluster aggregation models, while providing useful first approximations, are unable to describe these aggregate populations, not only with respect to H (this paper) but also with respect to first-order lacunarity (25, 26). It is concluded that the affinity exponent gives a more detailed description of such aggregates than the mass fractal dimension taken alone, and is expected to be useful for practical applications, in particular for more accurately predicting coagulation dynamics, transport properties (e.g., Brownian diffusivity) and the kinetics of morphological changes (see below). Additionally, while we have explicitly demonstrated these morphological regularities for a large population of *carbonaceous* soot aggregates, it is expected that these morphological characteristics carry over to many other *inorganic* flame-generated aggregates, e.g., Al_2O_3 via $Al(CH_3)_3$-seeded CH_4/N_2 flames because of similar fractal dimensions and first-order lacunarities (15, 26).

In addition to the fractal dimensions, lacunarities of the first and second order are defined as prefactors in the scaling relationships among aggregate mean mass, rms mass, and linear size. Lacunarities are useful to classify the density and crossover scales of the samples having the same scaling exponents. Analysis of the second moment of the mass-size distribution demonstrated that the scaling properties of aggregates can not be adequately characterized by a single

fractal dimension; rather, it is necessary to introduce a set of scaling exponents. It remains to be determined what level of description will be necessary or adequate for each of the aggregate properties (mobility, restructuring, kinetics, etc.) of interest here. However, our premise remains that a more precise characterization of aggregate morphologies in terms of self-affine scaling and lacunarities, presently not captured by idealized cluster–cluster aggregation models, will lead to an improved description of the coagulation dynamics, transport properties and restructuring kinetics of flame-generated and other disordered ''asymmetric'' aggregates.

ACKNOWLEDGMENTS

This research was sponsored in part by AFOSR Grant 94-1-0143 with J. M. Tishkoff serving as Technical Monitor, the Yale HTCRE Laboratory Industrial Affiliates (DuPont and ALCOA), and the Mandelbrot Foundation for Fractals. The authors also acknowledge valuable discussions with Dr. Benoit B. Mandelbrot.

REFERENCES

1. Mandelbrot, B. B., ''The Fractal Geometry of Nature.'' Freeman, New York, 1983.
2. Jullien, R., and Botet, R., ''Aggregation and Fractal Aggregates.'' World Scientific, Singapore, 1987.
3. Vicsek, T., ''Fractal Growth Phenomena.'' World Scientific, Singapore, 1992.
4. Witten, T. A., and Sander, L. M., *Phys. Rev. Lett.* **47,** 1400 (1981).
5. Brady, R. M., and Ball, R. C., *Nature (London)* **309,** 225 (1984).
6. Feder, J., ''Fractals.'' Plenum, New York, 1988.
7. Honjo, H., Ohta, S., and Matsushita, M., *J. Phys. Soc. Jpn.* **55,** 2487 (1986).
8. Elam, W. T., Wolf, S. A., Sprague, J., Gubser, D. U., Van Vechten, D., Barz, G. L., and Meakin, P., *Phys. Rev. Lett.* **54,** 701 (1985).
9. Kaufman, J. H., Baker, C. K., Nazzal, A. I., Flinker, M., and Melroy, O. R., *Phys. Rev. Lett.* **56,** 1932 (1986).
10. Niemeyer, L., Pietronero, L., and Wiesmann, A. J., *Phys. Rev. Lett.* **52,** 1033 (1984).
11. Daccord, G., *Phys. Rev. Lett.* **58,** 479 (1987).
12. Weitz, D. A., and Huang, J. S., *in* ''Kinetics of Aggregation and Gelation'' (F. Family and D. P. Landau, Eds.), p. 19. Elsevier, Amsterdam, 1984.
13. Forest, S. R., and Witten, T. A., *J. Phys. Rev. A* **12,** 109 (1979).
14. Megaridis, C. M., and Dobbins, R. A., *Combust. Sci. Technol.* **71,** 95 (1990).
15. Xing, Y., Köylü, Ü. Ö., and Rosner, D. E., *Combust. Flame*, in press.
16. Samson, R. J., Mulholland, G. W., and Gentry, J. W., *Langmuir* **3,** 272 (1987).
17. Lin, M. Y., Lindsay, H. M., Weitz, D. A., Ball, R. C., Klein, R., and Meakin, P., *Proc. Roy. Soc. London Ser. A* **423,** 71 (1989).
18. Hasmy, A., Foret, M., Pelous, Y., and Jullien, R., *Phys. Rev. B* **48,** 9345 (1993).
19. Lushnikov, A. A., Maksimenko, V. V., and Pakhomov, A. V., *J. Aerosol Sci.* **20,** 865 (1990).
20. Ehrburger-Dolle, F., Misono, S., and Lahaye, Y., *J. Colloid Interface Sci.* **135,** 468 (1990).
21. Aubert, C., and Connell, D. S., *Phys. Rev. Lett.* **56,** 738 (1986).
22. Sorensen, C. M., Cai, J., and Lu, N., *Appl. Opt.* **31,** 6547 (1992).
23. Puri, R., Richardson, T. F., Santoro, R. J., and Dobbins, R. A., *Combust. Flame* **92,** 320 (1993).
24. Cai, J., Lu, N., and Sorensen, C. M., *J. Colloid Interface Sci.* **171,** 470 (1995).
25. Köylü, Ü. Ö., Faeth, G. M., Farias, T. L., and Carvalho, M. G., *Combust. Flame* **100,** 621 (1995).
26. Köylü, Ü. Ö., Xing, Y., and Rosner, D. E., *Langmuir* **11,** 4848 (1995).
27. Botet, R., and Jullien, R., *J. Phys. A: Math. Gen.* **19,** L907 (1986).
28. Lindsay, H. M., Klein, R., Weitz, D. A., Lin, M. Y., and Meakin, P., *Phys. Rev. A* **39,** 3112 (1989).
29. Köylü, Ü. Ö., and Faeth, G. M., *Combust. Flame* **89,** 140 (1992).
30. Köylü, Ü. Ö., and Faeth, G. M., *ASME J. Heat Trans.* **116,** 971 (1994).
31. Sunderland, P. B., Köylü, Ü. Ö., and Faeth, G. M., *Combust. Flame* **100,** 310 (1995).
32. Dobbins, R. A., and Megaridis, C. M., *Langmuir* **3,** 254 (1987).
33. Rosner, D. E., Mackowski, D. W., and Garcia-Ybarra, P., *Combust. Sci. Technol.* **80,** 87 (1991); see, also, Garcia-Ybarra, P., and Rosner, D. E., *AIChEJ.* **35,** 139.
34. Mandelbrot, B. B., *Phys. Scr.* **32,** 257 (1985).
35. Mandelbrot, B. B., *in* ''Fractals in Physics'' (L. Pietronero and E. Tosatti, Eds.). Elsevier, Amsterdam, 1986.
36. Neimark, A. V., *Phys. Rev. B* **50,** 15435 (1994).
37. Stahl, W. R., *Science* **137,** 205 (1962).
38. Galileo, G., ''Dialogues Concerning Two New Sciences,'' 1638 (see ''Dimensional Methods and Their Applications.'' Arnold, London, 1953).
39. Rosner, D. E., and Tandon, P., *AIChE J.* **40,** 1167 (1994).
40. Tandon, P., and Rosner, D. E., *Ind. Eng. Chem. Res.* **34,** 3265 (1995).
41. Loewenberg, M., and O'Brien, R. W., *J. Colloid Interface Sci.* **150,** 158 (1992).
42. Kasper, G., Nida, T., and Yang, M., *Aerosol Sci.* **16,** 515 (1985).
43. Davis, R. H., *Phys. Fluids A* **3,** 2051 (1991).
44. Mackowski, D. W., *J. Colloid Interface Sci.* **140,** 138 (1990).
45. Garcia-Ybarra, P., and Rosner, D. E., *AIChE J.* **35,** 139 (1989).
46. Tandon, P., and Rosner, D. E., *Chem. Eng. Commun.*, in press.